crystals

MDPI

Article

Synthesis, Crystal Structure and Solid State Transformation of 1,2-Bis[(1-methyl-1*H*-imidazole-2-yl)thio]ethane

Leo Štefan [1,*], Dubravka Matković-Čalogović [2], Darko Filić [3] and Miljenko Dumić [4]

1 JGL d.d., Jadran Galenski Laboratorij, 51000 Rijeka, Croatia
2 Department of Chemistry, Faculty of Science, University of Zagreb, 10000 Zagreb, Croatia; dubravka@chem.pmf.hr
3 Fidelta d.o.o., 10000 Zagreb, Croatia; darko.filic@fidelta.eu
4 Department of Biotechnology, University of Rijeka, 51000 Rijeka, Croatia; mdumic@biotech.uniri.hr
* Correspondence: leo.stefan@jgl.hr; Tel.: +385-98-214-996

Received: 13 July 2020; Accepted: 28 July 2020; Published: 3 August 2020

Abstract: The spontaneous *S*-alkylation of the thyreostatic drug methimazole (1-methyl-1,3-dihydro-1*H*-imidazole-2-thione, **1**) with 1,2-dichloroethane at room temperature, in dark or light conditions, led to the formation of its related substance 1,2-bis[(1-methyl-1*H*-imidazole-2-yl)thio]ethane, $C_{10}H_{14}N_4S_2$ (**2a**), primarily isolated in the form of dihydrochloride tetrahydrate $[C_{10}H_{16}N_4S_2]Cl_2{\cdot}4(H_2O)$ (**2b**), which crystallized in the monoclinic $P2_1/c$ space group. Neutralization of **2b,** followed by crystallization from the acetone/water mixture, produced dihydrate $C_{10}H_{14}N_4S_2{\cdot}2(H_2O)$ (**2c**), which crystallized in the trigonal *R*-3 space group. Six water molecules in **2c** are H-bonded mutually and to the nitrogen atoms of six molecules of **2a.** DSC and TGA showed that **2c** melts at 65 °C and loses water up to 120 °C. By cooling to room temperature, anhydrous **2a** was obtained. Single crystals of **2a** that are suitable for X-ray structure analysis were obtained by neutralization of **2b,** followed by crystallization from dry dichloromethane. Anhydrous **2a** crystallizes in the monoclinic $P2_1/c$ space group. The dehydration of **2c** led to the formation of the anhydrous product **2a,** which is identical to the one obtained by crystallization, as was found by complementary solid-state techniques. No intermediate monohydrate or hemihydrate phases were detected. Powder diffraction showed the same pattern of **2c** via both preparation procedures. The structures of all the forms were elucidated by spectroscopy, microscopy and thermal methods and confirmed by single crystal X-ray analysis.

Keywords: methimazole; 1,2-bis[(1-methyl-1*H*-imidazole-2-yl)thio]ethane; solid-state forms; hydrates; dehydration

1. Introduction

Methimazole (1-methyl-1,3-dihydro-1*H*-imidazole-2-thione, **1**), a well-known commercially available thyreostatic drug [1], has an ambidentate heterocyclic anion of the type [N-C-S] and was used as the terminal group in the synthesis of noncyclic crown ethers as scorpionate ligands in diverse aspects of the coordination chemistry [2,3].

Among the bridged bis(methimazole) compounds, 1,2-bis[(1-methyl-1*H*-imidazole-2-yl)thio]methane (**A**) and an analogous ethane derivative 1,2-bis[(1-methyl-1*H*-imidazole-2-yl)thio]ethane (**2a**) were synthesized from **1** and dichloromethane or 1,2-dibromoethane. Synthesis was performed in the presence of a strong base, without or under phase-transfer conditions at an elevated temperature [4,5]. In the context of the pharmaceutical purity profile, these compounds are considered as potential methimazole related substances [6], especially if common solvents, e.g., dichloromethane (DCM) and 1,2-dichloroethane (DCE), are used in the synthetic transformations, isolation, purification and methimazole analytics.

Therefore, it was important to understand their behaviour from a chemical, structural and solid-state point of view. To evaluate these factors, we carried out a preliminary stability study of **1** in DCM and DCE in daylight or dark, at ambient humidity and room temperature.

2. Results and Discussion

2.1. Synthesis of Bis Derivative 2

Solutions of **1** in DCM or DCE were left without stirring in daylight or dark, at ambient humidity and at room temperature for 15 days. According to the TLC analysis, no changes of **1** were observed in DCM solutions. However, in both DCE solutions (i.e., in light and dark) spontaneous S-bis alkylation of **1** by 1,2-dichloroethane led to the formation of colourless plate shaped crystals of 1,2-bis[(1-methyl-1*H*-imidazole-2-yl)thio]ethane in the form of dihydrochloride tetrahydrate (**2b**) with a 30% yield; mp. (DSC, onset): 208 °C. Purity by HPLC: 98%. Upon its neutralization, extraction, evaporation of the solvent and crystallization of the crude residue from the dry dichloromethane under low humidity conditions of the anhydrous 1,2-bis[(1-methyl-1*H*-imidazole-2-yl)thio]ethane **2a** was obtained with an 84% yield, mp. (DSC, onset): 89 °C (lit: 88–90 °C, [5]).

However, if crystallization of the crude residue is attempted from the acetone/water (1/1) mixture, 1,2-bis[(1-methyl-1*H*-imidazole-2-yl)thio]ethane dihydrate (**2c**) is obtained with a 78% yield; mp. (DSC, onset): 65 °C. The same product was obtained by the crystallization of pure **2a** from the acetone/water (1/1) mixture. Anhydrous from **2a** was also prepared by drying the dihydrate **2c** (Scheme 1).

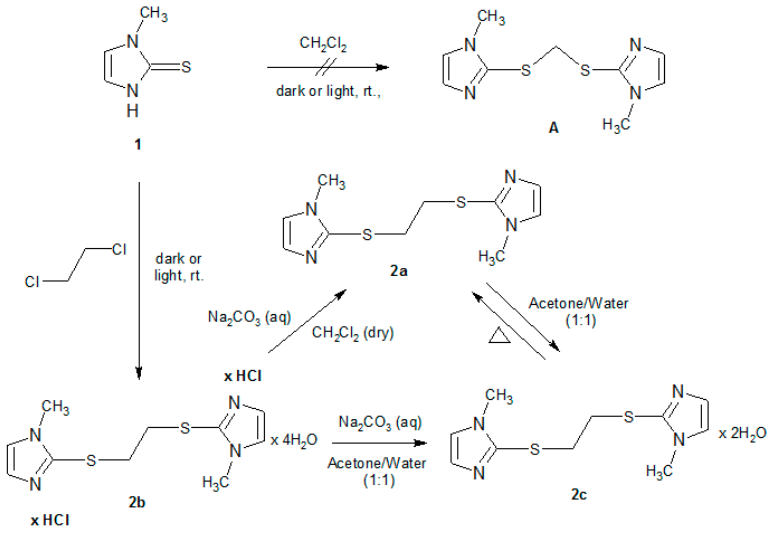

Scheme 1. Synthesis of 1,2-bis[(1-methyl-1*H*-imidazole-2-yl)thio]—derivatives **A** and **2** (**2a**–**2c**).

2.2. Characterization of 1,2-Bis[(1-methyl-1H-imidazole-2-yl)thio]ethane Forms 2a–2c

All the studied forms, **2a**–**2c**, were elucidated using spectroscopy, microscopy, thermal and complementary analytical methods. Their structures were confirmed by the single crystal X-ray diffraction analysis.

Proton chemical shifts of dihydrochloride tetrahydrate **2b**, recorded in D_2O, were different in comparison to the previously reported data for **2a** in $CHCl_3$-C_6H_6 [5], while relative integrations indicated protonation of the imidazole ring and confirmed the proposed structure (Figure 1). Mass spectra recorded in the positive mode indicated the most abundant ion at 255.0743 m/z, which was attributed to the base peak of **2a,** corresponding to $[M+H-2HCl]^+$. Additionally, two formed fragments at 141.0486 m/z and 114.0249 m/z indicated cleavage of the thioethyl group. However, DSC showed an endothermic loss of volatile solvents between 35 and 70 °C. In addition, mass loss by TGA of 3.8% and chloride content of 18%, determined by ionic chromatography, indicated that

the product crystallized as a dihydrochloride tetrahydrate. The hypothesis was confirmed by single crystal X-ray diffraction analysis.

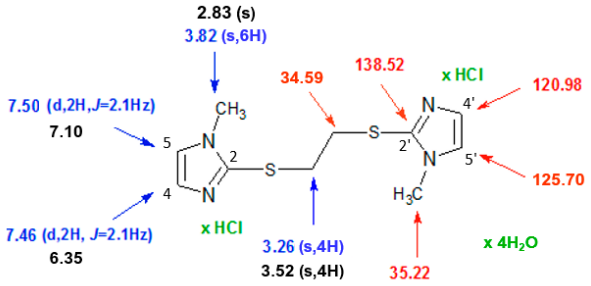

Figure 1. ^{1}H (600 MHz) (blue), ^{13}C (151 MHz) (red) NMR in D_2O of **2b** and ^{1}H (black) NMR in $CDCl_3$-C_6D_6 of **2a** [5].

The molecular structure of **2b** consisted of two cationic imidazolyl groups bounded to the *S*-atoms of the dithioethyl group (Figure 2a). Each chloride anion was a hydrogen bond acceptor from the protonated imidazole nitrogen atom N2 and two water molecules (Figure 2b, Table 1). The two water molecules were also connected by hydrogen bonds. Through these hydrogen bonds, the cations, chloride anions and water molecules were interconnected into a 3D network.

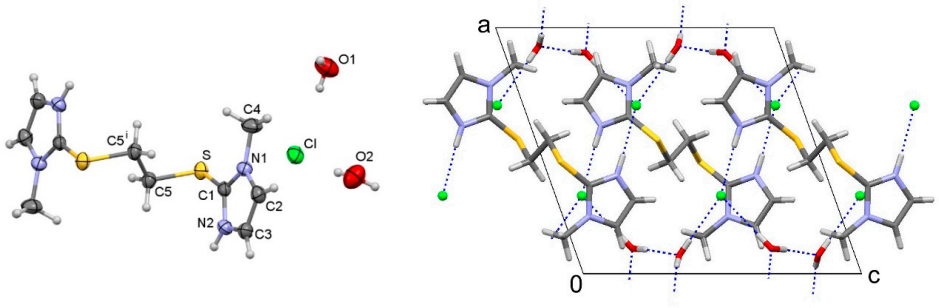

(**a**) (**b**)

Figure 2. (**a**) Molecular structure of **2b** with the atomic numbering scheme; symmetry code (i) 1 − x, −y, −z, and (**b**) packing diagram of **2b** viewed along the *b*-axis. Hydrogen bounds are marked by dashed blue lines.

Table 1. Distances and angles of the hydrogen bonds in **2b** and **2c**.

Form	Donor-H···Acceptor	*d*(D-H)/Å	*d*(H-A)/Å	*d*(D···A)/Å	<*d*(D-H···A)/°
2b	N2-H2···Cl [a]	0.86	2.26	3.112 (2)	172
	O1-H11···O2 [b]	0.78 (4)	1.98 (4)	2.749 (5)	169 (5)
	O1-H12···Cl [c]	0.75 (5)	2.44 (5)	3.190 (4)	178 (6)
	O2 -H21···Cl	0.78 (6)	2.42 (6)	3.198 (4)	174 (5)
	O2 -H22···O1	0.83 (3)	1.93 (3)	2.756 (5)	172 (3)
2c	O1-H1···N2 [d]	0.81 (3)	2.03 (3)	2.827 (3)	167 (4)
	O1-H12···O1 [e]	0.87 (4)	1.92 (4)	2.787 (4)	176 (4)
	C4-4B···O1 [f]	0.96	2.58	3.489 (4)	157

Transformation of the asymmetric unit: (**a**) 1 − x, −1/2 + y, 1/2 − z; (**b**) −x, 1/2 + y, 1/2 −z; (**c**) x, 3/2 − y, 1/2 + z; (**d**) −x + y, −x, z; (**e**) y, −x + y, −z; (**f**) 1/3 − x + y, 2/3 −x, −1/3 + z.

Proton and carbon chemical shifts in the NMR spectra of **2a** in DMSO-d6 exhibited similar values to those in **2b**, and experimental MS data matched the theoretical data. After several attempts, we obtained good quality, single crystals by crystallisation from dry dichloromethane at dry conditions (see experimental section) that allowed us to confirm the anhydrous structure of **2a**, which crystallized in the monoclinic $P2_1/c$ space group.

There are no hydrogen bounds in the structure of **2a**, only van der Waals forces connect the molecules (Figure 3).

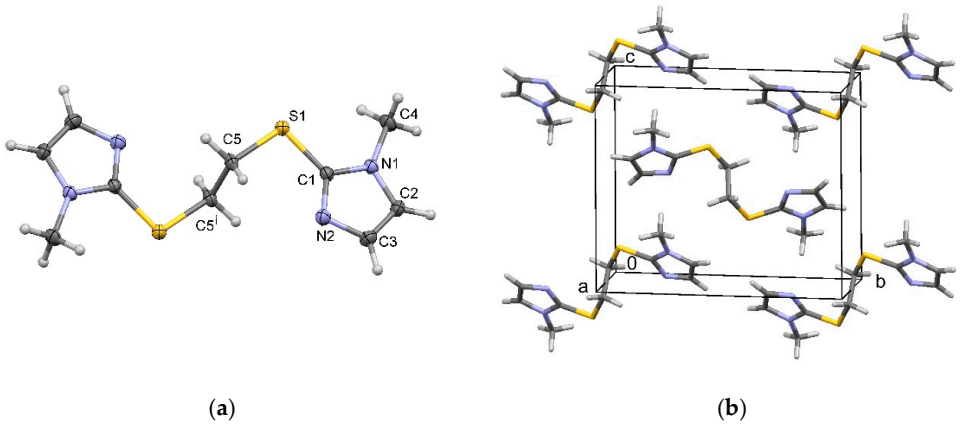

(**a**) (**b**)

Figure 3. (**a**) Molecular structure of **2a** with the atomic numbering scheme; symmetry code (i) 1 − x, −y, −z, and (**b**) packing diagram of **2a**.

Crystals of **2c** showed the TLC Rf value of 0.59, which was the same as **2a** and **2b**, and a TGA volatile content of 11.31%, indicating the solvated form of the same substance. The structure was solved by the single crystal X-ray diffraction analysis, showing that the dihydrate **2c** crystallizes in the trigonal *R* -3 space group. Six water molecules were mutually interconnected by hydrogen bonds, forming a hexagon in the chair conformation, which is the most common conformation for a cluster of six water molecules. The R6 motif is usually formed by water molecules related by a centre of symmetry [7]. In **2c**, one water molecule formed the R6 pattern by the -3 symmetry element ($R_6^6(12)$ by the graph-set notation). The water molecule was an acceptor of a hydrogen bond from N2 and a weak one from C4, thus forming a 3D network (Figure 4, Table 1).

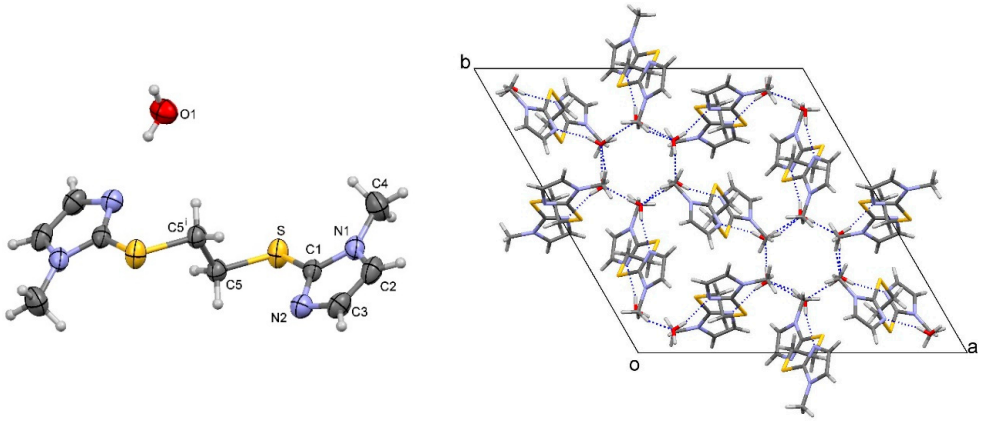

(**a**) (**b**)

Figure 4. (**a**) Molecular structure with the atomic numbering scheme; symmetry code (i) 2/3 − x, 1/3 − y, 4/3 − z, and (**b**) packing diagram of **2c** viewed along the *c*-axis. Hydrogen bonds are marked with blue dashed lines.

The molecular structure of 1,2-bis[(1-methyl-1*H*-imidazole-2-yl)thio]ethane consisted of two imidazole groups bounded to the S-atoms of the dithioethyl group (**2a**, **2c**). The imidazole groups were protonated in **2b**. In all three structures, the ethane moiety lied at the centre of symmetry, and thus only half of the molecule was in the asymmetric unit. Therefore, the imidazole groups were parallel. The difference in the three structures was found in the orientation of the imidazole group, i.e., rotation

about the S-C1 bond resulting in different C5-S-C1-N1 torsion angles (−173.8(2)°, −113.4(2)° and 151.8(2)°, in **2a**, **2b** and **2c,** respectively (Figure 5).

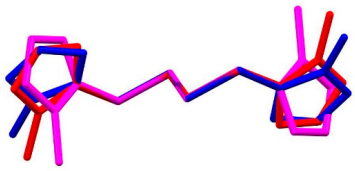

Figure 5. Molecule overlay of **2a** (blue), **2b** (magenta) and **2c** (red). Atoms C5 and S and their pairs related by the inversion centre were used for the overlay. Hydrogen atoms are omitted for clarity.

2.3. Dehydration Behaviour of Dihydrate 2c and Its Transformation to the Anhydrous Form 2a

Hydrates are the most common type of solvated organic compounds [8], and understanding their dehydration pathways, as a widespread but not properly understood phenomenon, is critical for designing optimal properties for materials, particularly in the case of pharmaceutical solids [9]. Several schemes for the classification of hydrates have been proposed [10–13], but in general, dehydration results in three types of crystallographic behaviour: a) material where the crystal structure changes (different powder pattern) after dehydration, i.e., as in the present study, contrary to b) material that undergoes only a slight change in crystal structure (related XRPD pattern) after dehydration, like some azithromycin solvates [14], or c) material that becomes amorphous after dehydration, like some other azithromycin solvates [15].

The dehydration process of **2c** had a markedly different crystal structure of the anhydrous form **2a** and has been studied using different experimental techniques. The dihydrate **2c** was heated below the melting point, at around 55 °C and at reduced pressure of 200 mbar to a constant mass. A significant rate of the dehydration process was detected after 30 min by the formation of opaque crystals. The process was completed after 60 min.

DSC measurement of the selected samples showed, after 30 min, endothermic events belonging to the melting of **2c** and **2a**, indicating the coexistence of both forms in the sample (Figure 6, iii), and finally, after 60 min, only a single endothermic event at 90 °C, belonging to the melting of the anhydrous form **2a** (Figure 6, iv). Unfortunately, no sign of recrystallization was detected.

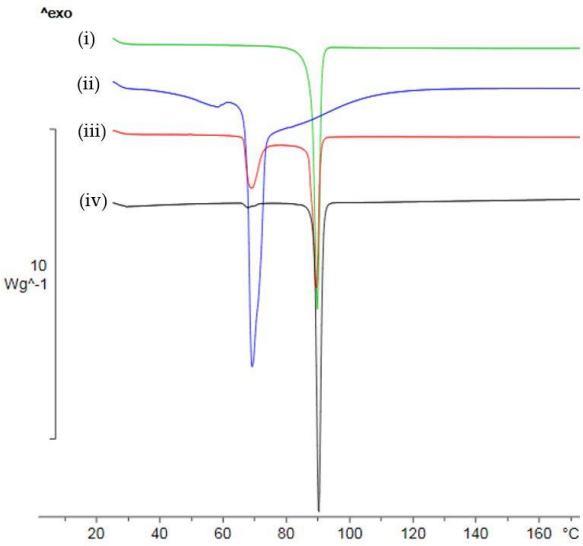

Figure 6. Selected DSC thermograms showing solid state transformation of the dihydrate **2c** to the anhydrous form **2a** recorded under a heating rate of 10 °C/min and N_2 purge in a pierced lid crucible; (i) anhydrous form **2a**; (ii) dihydrate **2c**; (iii) product after heating **2c** at 55 °C/200 mbar for 30 min, and (iv) product after heating **2c** at 55 °C/200 mbar for 60 min.

Finally, the XRPD powder pattern of the dried sample was different from the powder pattern of dihydrate **2c** and identical to the calculated powder pattern of anhydrous **2a** prepared by crystallization (Figure 7), confirming that **2a** is also the final product of dihydrate **2c** dehydration.

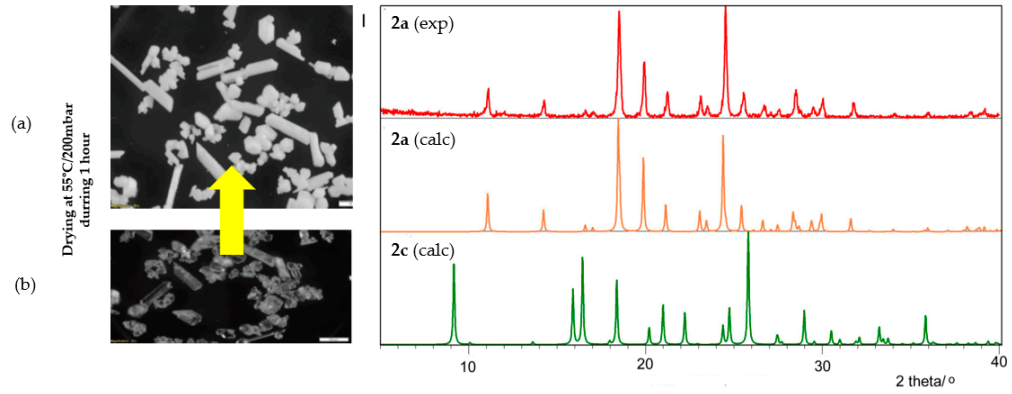

Figure 7. Photomicrographs of: (**a**) anhydrous **2a** after drying of **2c** during 60 min at 55 °C /200mbar; (**b**) starting dihydrate **2c** and the related PXRD patterns.

Additional studies were performed under atmospheric pressure to determine whether dehydration of **2c** to **2a** proceeds via a metastable monohydrate intermediate, as in lisinopril dihydrate [16], or as a hemihydrate, such as ondansetron hydrochloride dihydrate [17].

The TGA thermogram of **2c** showed a single thermal event in the range 40–110 °C with a mass loss of 11.31%, corresponding to the loss of two water molecules. This was in agreement with the DSC thermogram showing only a sharp endothermic event with an onset at 65 °C, corresponding to the melting of **2c**. Additional exothermic processes of recrystallization and endothermic of melting were not detected (Figure 8).

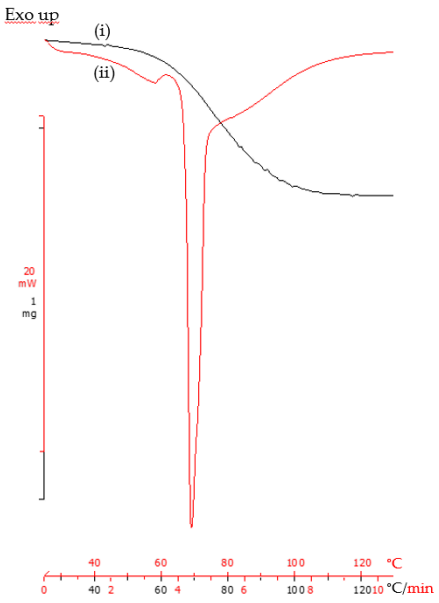

Figure 8. TGA (i) and DSC (ii) analysis of dihydrate **2c** in perforated crucibles under a heating rate of 10 °C/min and N_2 purge.

The changes upon dehydration of **2c** were monitored by the combination of hot stage microscopy (HSM) with DSC at a heating/cooling rate of 10 °C/min (Figure 9). Melting started at 40 °C until completed at around 65 °C (step i). Immediately after the melting point, the melt of **2c** was cooled to room temperature, resulting in a glassy product, and no further crystallisation was observed

after prolonged standing. However, if **2c** was heated to 80 °C and immersed in oil during the HSM experiment, followed by cooling, recrystallization of the dihydrate **2c** was observed due to the conditions that inhibited efficient water removal. However, if the sample was heated over melting, up to 95 °C, in an open pan followed by cooling to room temperature, spontaneous crystallisation occurred, and according to XRPD, the obtained product was a mixture of the dihydrate **2c** and the anhydrous form **2a**.

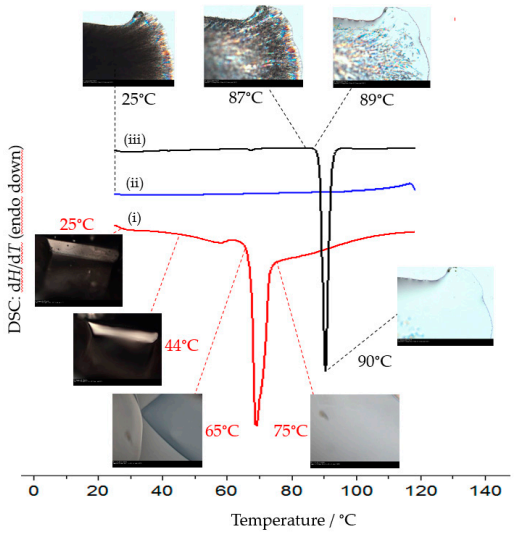

Figure 9. Selected DSC thermograms and HSM micrographs of dihydrate **2c,** recorded using a heating/cooling rate of 10 °C/min with perforated DSC crucibles: (i) dihydrate **2c** heating step up to 120 °C; (ii) cooling step to room temperature, and (iii) heating step of the recrystallized anhydrous form **2a**, i.e., re-run (re-heating) of the sample in the bottom thermogram.

In contrast, when the melt of **2c** was heated to 120 °C and cooled to room temperature, according to the XRPD slow nucleation and growth process of the anhydrous form **2a** occurred after prolonged standing indicating complete dehydration (step ii). In the re-run the sample melting started at 89 °C until completed at around 90 °C (step iii), i.e., at the melting point of the anhydrous form **2a**. However, no additional exothermic and endothermic events or changes in XRPD, which could indicate the formation of potential intermediary monohydrate or hemihydrate phases, were observed.

Dehydration of **2c** in vacuo favours rapid water removal below the melting point, without the appearance of a liquid or melt phase. Removal of water molecules from **2c** under these conditions resulted in the solid-solid rearrangement of the molecules in the crystal lattice, leading to anhydrous **2a**. On the contrary, crystallization of **2a** from the melt of dihydrate **2c** under atmospheric pressure only occurred when all the residual water was removed from the sample (at 120 °C). When a sample of melted **2c** was only heated to 95 °C, concomitant crystallization of **2a** and **2c** was observed, and this was identical to the partial dehydration of **2c** after 30 min under reduced pressure.

Finally, we can conclude that the dehydration at both conditions, i.e., under reduced and atmospheric pressure, proceeds to the anhydrous form **2a** and it is in accordance with the well-known fact that dehydration processes are greatly dependent on the atmospheric environment [11,18].

3. Materials and Methods

3.1. General

Methimazole **1** 99%, Ph Eur quality, was purchased from CU Chemie Ueticon, Lahr, Germany (water content 0.4%), 1,2-dichloroethane (Fisher, Hampton, NH, USA) (water content, 0.02%), dichloromethane (Merck KGaA, Darmstadt, Germany) acetone (Sigma, St. Louis, MO, USA) (water content, 0.2%), methanol dried (Merck KGaA, Darmstadt, Germany), water was purified in a house system (Thornton

2000CRS, Mettler Toledo, Colombus, OH, USA) and was of HPLC grade. Dichloromethane was dried under anhydrous sodium sulphate and distilled prior to use. All other used chemicals were of analytical grade. pH measurements were performed using Mettler Toledo (Columbus, OH, USA) Seven Multi pH meter, and prior to measurement, it was calibrated in six points. Ionic chromatography measurements were performed on Thermo (Waltham, MA, USA) ionic chromatography using LC chlorine standard. HPLC analysis was performed on an Agilent Technologies (Santa Clara, CA, USA) HPLC instrument under gradient elution at a flow rate of 0.6 mL/min using mobile phase A (ammonium acetate, Merck KGaA, Darmstadt, Germany buffer) and mobile phase B (acetonitrile, Merck KGaA, Darmstadt, Germany) at the Zorbax C18 column. The effluent was monitored using the Agilent DAD/UV detector. ^{1}H NMR and ^{13}C NMR spectra were recorded on a Bruker (Billerica, MA, USA) Advance 600 and 150, respectively, with DMSO-*d6* or D_2O as a solvent. Mass spectra were recorded on an Agilent 6550 iFunnel quadrupole time-of-flight mass spectrometer equipped with dual AJS ESI source (Agilent Technologies Santa Clara, CA, USA). Hot stage microscopy was carried out using an Olympus (Shinjuku City, Tokyo, Japan) BX51 microscope combined with a Linkam THMS 600 hot stage (Linkam Scientific Instruments, Waterfield, UK) and a digital camera (QImaging, Surrey, Canada) for image capture. A small amount of the sample was placed onto a glass slide and viewed with 100x magnification and partially polarised light. It was simultaneously being heated from ambient temperature at a rate of 10 °C/min. Thermal analysis was performed using a Mettler DSC 1 instrument (Mettler Toledo, Greifensee, Swizerland) in aluminium pans with a pierced lid at a heating rate of 10 °C/min under the inert nitrogen atmosphere with a flow rate of 55 mL/min. Temperature calibration was performed using the indium metal standard. TGA data were collected on a Mettler Toledo (Greifensee, Switzerland)) TGA/SDTA 851e system. The sample was loaded onto a pre-tared alumina crucible and was heated at a heating rate 10 °C/min over the temperature range 25–300 °C. A nitrogen purge at 50 mL/min was maintained over the sample. The instrument was temperature calibrated using certified $NiMn_3Al$ and nickel. All weighing operations were carried using Mettler Toledo (Greifensee, Switzerland)) balance, daily calibrated according to the internal program.

3.2. Synthesis of 1,2-Bis[(1-methyl-1H-imidazole-2-yl)thio]ethane Dihydrochloride Tetrahydrate (2b)

Method (A) Methimazole (100 mg, 0.87 mmol) was dissolved in 10 mL of 1,2-dichloroethane. The solution was left without stirring for 15 days in the dark at room temperature in a humidity non-controlled environment. The precipitated product was collected using vacuum suction and rinsed few times with cold 1,2-dichloroethane, yielding 1,2-bis[(1-methyl-1*H*-imidazole-2-yl)thio]ethane dihydrochloride tetrahydrate (**2b**, 53 mg, 31%) in the form of colourless plate shape crystals. Melting point (DSC, onset): 208 °C, MS-QTOF: $[M+H-2HCl]^+$ 255.0743, [M-2HCl] 254.066, $C_{10}H_{14}N_4S_2$. ^{1}H NMR (D_2O, 600 MHz/ppm): N-CH_3 (s, 6H), 3.82, H-C4 (d, 2H) 7.46, J = 2.1 Hz, H-C5 (d, 2H) 7.50, J = 2.1 Hz, S-CH_2 (s, 4H) 3.26. ^{13}C NMR (D_2O, 151 MHz/ppm): N-CH_3 35.22, C4 120.98, C5 125.70, C2 138.52, S-CH_2 34.59, Purity (HPLC): 98%, RRT: 20.518. Ionic chromatography: experimentally determined percentage of Cl ions (19%) corresponded to the theoretical value (18%) within the experimental error. The structure of **2b** was confirmed by single crystal X-ray diffraction analysis.

Method (B) Methimazole (100 mg, 0.87 mmol) was dissolved in 10 mL of 1,2-dichloroethane. The solution was left without stirring for 15 days in daylight and room temperature in a humidity non-controlled environment. The precipitated product was collected using vacuum suction and rinsed a few times with cold 1,2-dichloroethane, yielding dihydrochloride tetrahydrate **2b** (52 mg, 30%) in the form of colourless plate shaped crystals. Melting point (DSC, onset): 208 °C. The NMR spectra and XRPD diffractogram of the prepared sample were identical to the spectra and diffractogram of the **2b** sample obtained by Method A.

3.3. Synthesis of Anhydrous 1,2-Bis[(1-methyl-1H-imidazole-2-yl)thio]ethane (2a)

Method (A) Dihydrochloride tetrahydrate **2b** (300 mg) was dissolved in 30 mL of water and neutralized with 1M Na_2CO_3 to pH 7.0, followed by extraction with dichloromethane (3 × 10 mL),

washed with brine and dried with anhydrous Na_2SO_4. Evaporation of the solvent in vacuo to dryness yielded crude 1,2-bis[(1-methyl-1*H*-imidazole-2-yl)thio]ethane (**2a**, 160 mg, 84%) in a form of white powder. Recrystallization of dry crude **2a** from dry dichloromethane under low humidity conditions gave pure anhydrous **2a**. Melting point (DSC, onset): 89 °C (lit: 88-90 °C) [5], ^{1}H NMR (DMSO-*d6*, 600 MHz/ppm): N-CH_3 (s, 6H) 3.57, H-C4 (d, 2H) 7.24 *J* = 1.2 Hz, H-C5 (d, 2H) 6.94 *J* = 1.2 Hz, S-CH_2 (s, 4H) 3.21; ^{13}C NMR (DMSO-*d6*, 151 MHz/ppm): N-CH_3 32.79, C4 123.29, C5 128.53, C2 139.23, S-CH_2 33.30. The structure of **2a** was confirmed by single crystal X-ray diffraction analysis.

Method (B) Dihydrate **2c** (100 mg) was dried under reduced pressure of 200 mbar at 55 °C for 60 min and anhydrous form **2a** (71 mg, 81%) was obtained. DSC thermogram and XRPD diffractogram of the obtained sample were identical to the thermogram and diffractogram of the **2a** sample obtained by Method A.

3.4. Synthesis of 1,2-Bis[(1-methyl-1H-imidazole-2-yl)thio]ethane Dihydrate (2c)

Method (A) Crude **2a** obtained by neutralization of dihydrochloride tetrahydrate **2b** (160 mg) was dissolved in an acetone/water mixture (1:1). After prolonged standing of the solution without stirring at room temperature, crystals of the pure dihydrate form **2c** (133 mg, 73%) were obtained. Melting point (DSC, onset, 65 °C). Structure of **2c** was confirmed by the single crystal X-ray diffraction analysis.

Method (B) Pure anhydrous form **2a** (300 mg) was dissolved in an acetone/water mixture (1:1). After prolonged standing of the solution without stirring at room temperature, pure crystals of the dihydrate form **2c** (238 mg, 70%) were obtained. DSC thermogram and XRPD diffractogram of the so obtained sample were identical to the thermogram and diffractogram of the **2c** sample obtained by Method A.

3.5. Powder X-ray Diffraction

X-ray powder diffraction (XRPD) data were collected at room temperature using copper Kα radiation on a PANalytical X'Pert Pro powder diffractometer model PW3050/60 (PANalytical, Almelo, The Netherland) in Bragg-Brentano geometry equipped with a X'celerator detector. The sample was prepared by mounting a sample on a wafer (zero background) plate and scanned from 3 to 40° 2θ using the following acquisition parameters: generator tension 45 kV, generator current 40 mA, step size 0.0167°, scan speed 0.011°/second, number of steps 2214 and total collection time 60 min, scan speed 0.05°/second, number of steps 2214 and total collection time 13 min.

3.6. Single Crystal X-ray Diffraction Analysis and Structure Determination

Suitable single crystals were selected and mounted in air onto thin glass fibres. Diffraction data of **2b** and **2c** were collected at room temperature, while data from the anhydrous form **2a** were collected at 150 K on an Oxford Diffraction Xcalibur four-circle kappa geometry diffractometer with Xcalibur Sapphire 3 CCD detector, using graphite monochromated MoKα (λ = 0.71073 Å) radiation.

The essential crystallographic data from the solid forms **2a**, **2b** and **2c** are presented in Table 2.

Data reduction, correction for the Lorentz-polarization factor, scaling and multi-scan absorption correction was performed using the CrysAlisPro software package [19]. Solution, refinement and analysis of the structures were done using the programs integrated in the WinGX system [20]. The structures were solved by direct methods implemented in SHELXS [21,22]. Refinement by the full-matrix least-squares methods, based on F^2 against all reflections, was performed by SHELXL [21,22], including anisotropic displacement parameters for all non-H atoms. Hydrogen atoms bound to C and N (in **2b**) atoms were modelled by the riding model using the AFIX routine, while those bound to water oxygen atoms were located in the difference Fourier maps and refined isotropically. Analysis of the molecular geometry and hydrogen bonds was performed by PLATON [23]. The molecular graphics were done with MERCURY (Version 4.1.0) [24]. The crystal parameters, data collection and refinement results are summarized in Table 2. CCDC deposition numbers 2013658 (**2a**), 2013659 (**2b**) and 2013660 (**2c**) contain the supplementary crystallographic data for this paper. These data can be obtained free

of charge via http://www.ccdc.cam.ac.uk/conts/retrieving.html (or from the CCDC, 12 Union Road, Cambridge CB2 1EZ, UK; Fax: +44 1223 336033; E-mail: deposit@ccdc.cam.ac.uk)

Table 2. Essential crystallographic data for **2a**, **2b** and **2c**.

Compound	2a	2b	2c
Chemical formula	$C_{10}H_{14}N_4S_2$	$[C_{10}H_{16}N_4S_2]Cl_2{\cdot}4(H_2O)$	$C_{10}H_{14}N_4S_2{\cdot}2(H_2O)$
Formula weight	254.37	399.35	290.40
Crystal system	Monoclinic	Monoclinic	Trigonal
Space group	*P* 2_1/c	*P* 2_1/c	*R*–3
a/Å	4.7035 (7)	11.1667 (10)	19.3142 (13)
b/Å	12.3772 (14)	7.7629 (7)	19.3142 (13)
c/Å	10.3316 (11)	11.8970 (13)	10.3283 (5)
α/°	90	90	90
β/°	92.772 (14)	109.637 (11)	90
γ/°	90	90	180
Z	2	2	9
F (000)	268	420	1386
T/K	150	292	292
V/Å^3	600.76 (13)	971.32 (18)	3336.75 (5)
D_x /g.cm^3	1.406	1.365	1.301
S	0.933	0.900	1.047
R	0.0493	0.049	0.0398
wR (F^2)	0.1063	0.1272	0.0994
No. of reflections	972	2329	1448
CCDC	2013658	2013659	2013660

4. Conclusions

The presented research confirmed the great reactivity of methimazole in the 1,2-dichloroethane solution under mild conditions, leading to its spontaneous *S*-bis alkylation to 1,2-bis[(1-methyl-1*H*-imidazole-2-yl)thio]ethane in the form of dihydrochloride tetrahydrate (**2b**). Therefore, the use of 1,2-dichloroetane should be avoided when working with methimazole. Dihydrochloride tetrahydrate 2b, anhydrous **2a**, and dihydrate **2c** crystal forms were prepared and their structures were confirmed by the single crystal X-ray diffraction analysis. Dehydration process of the dihydrate **2c**, studied using complementary solid-state techniques, led to the formation of the anhydrous product **2a**, which was identical to the one obtained by crystallization. No intermediate monohydrate or hemihydrate phases were detected.

Author Contributions: Conceptualization, L.Š. and M.D.; investigation, L.Š., D.M.-Č., D.F.; data curation, L.Š., D.M.-Č., and M.D.; writing—original draft preparation L.Š. and M.D.; writing-review and editing L.Š., D.M.-Č., D.F. and M.D.; supervision M.D. All authors have read and agreed to the published version of the manuscript.

Funding: This research received no external funding.

Acknowledgments: The authors appreciate Lara Saftić Martinović (U. of Rijeka, Department for Biotechnology) for recording HR-MS spectra and deep discussion, Ivica Đilović (U. of Zagreb, Faculty of Science, Department of Chemistry) for single crystal data collection of 2a and Ana Čikoš (Institute Ruđer Bošković, Center for NMR, Zagreb) for recording NMR spectra and deep discussion.

Conflicts of Interest: The authors declare no conflict of interest.

References

1. Aboul-Enein, H.Y.; Al-Badr, A.A. Analytical Profile of Methimazole. In *Analytical Profiles of Drug Substances*; Florey, K., Ed.; Academic Press: New York, NY, USA, 1979; Volume 8, pp. 351–370.
2. Qingjian, L.; Mingli, S. Synthesis of noncyclic crown ethers with methimazole heterocycle as a terminal group. *Youji Huaxue* **1992**, *12*, 509–513.

3. Qingjian, L.; Mingli, S.; Chongqiu, J.; Fengling, L. Syntheses and coordination properties of bridged bis(methimazole) compounds. *Gaodeng Xuexiao Huaxue Xuebao* **1992**, *13*, 328–331.
4. Silva, R.M.; Smith, M.D.; Gardinier, J.R. Unexpected New Chemistry of the Bis(thioimidazolyl)methanes. *J. Org. Chem.* **2005**, *70*, 8755–8763. [CrossRef] [PubMed]
5. Hassanaly, P.; Dou, H.J.M.; Metzger, J.; Assef, G.; Kister, J.S. Alkylation of 2-Thioxo-2,3-dihydroimidazole and its 1-Methyl Derivative under Phase-Transfer Conditions. *Synthesis* **1997**, *4*, 253–254.
6. Pilaniya, K.; Chandrawanshi, H.K.; Pilaniya, U.; Manchandani, P.; Jain, P.; Singh, N. Recent trends in the impurity profile of pharmaceuticals. *J. Adv. Pharm. Technol. Res.* **2010**, *1*, 302–310.
7. Infantes, L.; Motherwell, S. Water clusters in organic molecular crystals. *Cryst. Eng. Comm.* **2002**, *4*, 454–461. [CrossRef]
8. Aaltonen, J.; Allesø, M.; Mirza, S.; Koradia, V.; Gordon, K.C.; Rantanen, J. Solid form screening—A review. *Eur. J. Pharm. Biopharm.* **2009**, *71*, 23–37. [CrossRef]
9. Larsen, A.S.; Ruggiero, M.T.; Johansson, K.E.; Zeitler, J.A.; Rantanen, J. Tracking Dehydration Mechanisms in Crystalline Hydrates with Molecular Dynamics Simulations. *Cryst. Growth Des.* **2017**, *17*, 5017–5022. [CrossRef]
10. Galwey, A.K. Structure and order in thermal dehydration of crystalline solids. *Thermochim. Acta* **2000**, *355*, 181–238. [CrossRef]
11. Petit, S.; Coquerel, G. Mechanism of Several Solid−Solid Transformations between Dihydrated and Anhydrous Copper (II) 8-Hydroxyquinolinates. Proposition for a Unified Model for the Dehydration of Molecular Crystals. *Chem. Mater.* **1996**, 2247–2258. [CrossRef]
12. Morris, K.R. Structural Aspects of Hydrates and Solvates. In *Polymorphism in Pharmaceutical Solids*; Brittain, H.G., Ed.; Marcel Dekker Inc.: New York, NY, USA, 1999; pp. 125–182.
13. Mimura, H.; Kitamura, S.; Kitagawa, T.; Kohda, S. Characterization of the non-stoichiometric and isomorphic hydration and solvation in FK041 clathrate. *Colloids Surf. B: Biointerfaces* **2002**, *26*, 397–406. [CrossRef]
14. Dumić, M.; Vinković, M.; Orešić, M.; Meštrović, E.; Danilovski, A.; Dumbović, A.; Knežević, Z.; Lazarevski, G.; Filić, D.; Cinčić, D.; et al. Isostructural Pseudopolymorphs of 9-Deoxo-9a-aza-9a-methyl-9a-homoerithromycin A. U.S. 7,569,549 B2, 4 August 2009.
15. Dumić, M.; Vinković, M.; Orešić, M.; Meštrović, E.; Danilovski, A.; Dumbović, A.; Knežević, Z.; Lazarevski, G.; Filić, D.; Cinčić, D.; et al. Novel Amorphous 9-Deoxo-9a-aza-9a-methyl-9a-homoerithromycin A, Process for Preparing the Same, and Uses Thereof. U.S. 6,936,591 B2, 30 August 2005.
16. Fujii, K.; Uekusa, H.; Itoda, N.; Yonemochi, E.; Terada, K. Mechanism of Dehydration–Hydration Processes of Lisinopril Dihydrate Investigated by ab Initio Powder X-ray Diffraction Analysis. *Cryst. Growth Des.* **2012**, *12*, 6165–6172. [CrossRef]
17. Mizoguchi, R.; Uekusa, H. Elucidating the Dehydration Mechanism of Ondansetron Hydrochloride Dihydrate with a Crystal Structure. *Cryst. Growth Des.* **2018**, *18*, 6142–6149. [CrossRef]
18. Byrn, S.R.; Pfeiffer, R.R.; Stowell, J.G. *Solid-State Chemistry of Drugs*, 2nd ed.; SSCI Inc.: West Lafayette, IN, USA, 1999; p. 292.
19. *CrysAlisPro Software System*, version 1.171.39.46; Rigaku Oxford Diffraction: Oxford, UK, 2018.
20. Farrugia, L.J. WinGX and ORTEP for Windows: An update. *J. Appl. Cryst.* **2012**, *45*, 849–854. [CrossRef]
21. Sheldrick, G.M. A short history of SHELX. *Acta Cryst.* **2008**, *64*, 112–122. [CrossRef] [PubMed]
22. Sheldrick, G.M. Crystal structure refinement with SHELXL. *Acta Cryst.* **2015**, *71*, 3–8.
23. Spek, A.L. Structure validation in chemical crystallography. *Acta Cryst.* **2009**, *65*, 148–155. [CrossRef] [PubMed]
24. Macrae, C.F.; Bruno, I.J.; Chisholm, J.A.; Edgington, P.R.; McCabe, P.; Pidcock, E.; Rodriguez-Monge, L.; Taylor, R.; Van De Streek, J.; Wood, P.A. *Mercury CSD 2.0*—New features for the visualization and investigation of crystal structures. *J. Appl. Cryst.* **2008**, *41*, 466–470. [CrossRef]